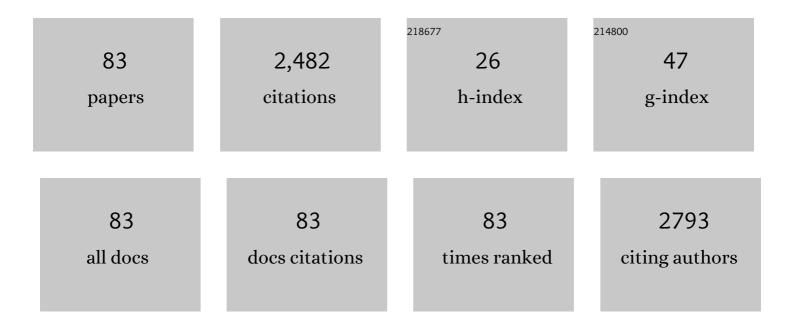
Hongyu An

List of Publications by Year in descending order

Source: https://exaly.com/author-pdf/698022/publications.pdf Version: 2024-02-01



Ηονοχή Δη

#	Article	IF	CITATIONS
1	A Path to Qualification of PET/MRI Scanners for Multicenter Brain Imaging Studies: Evaluation of MRI-Based Attenuation Correction Methods Using a Patient Phantom. Journal of Nuclear Medicine, 2022, 63, 615-621.	5.0	6
2	150 PET Imaging: Methods and Applications. , 2022, , 197-216.		0
3	Cerebral Oxygen Metabolic Stress is Increased in Children with Sickle Cell Anemia Compared to Anemic Controls. American Journal of Hematology, 2022, , .	4.1	10
4	<scp>MRâ€assisted PET</scp> respiratory motion correction using <scp>deepâ€learning</scp> based <scp>shortâ€scan</scp> motion fields. Magnetic Resonance in Medicine, 2022, 88, 676-690.	3.0	4
5	Oxygen Metabolic Stress and White Matter Injury in Patients With Cerebral Small Vessel Disease. Stroke, 2022, 53, 1570-1579.	2.0	19
6	Cranial vault imaging for pediatric head trauma using a radial VIBE MRI sequence. Journal of Neurosurgery: Pediatrics, 2022, 30, 113-118.	1.3	1
7	Silent Infarcts, White Matter Integrity, and Oxygen Metabolic Stress in Young Adults With and Without Sickle Cell Trait. Stroke, 2022, 53, 2887-2895.	2.0	5
8	Deepâ€learning synthesized pseudoâ€ <scp>CT</scp> for <scp>MR</scp> highâ€resolution pediatric cranial bone imaging (<scp>MRâ€HiPCB</scp>). Magnetic Resonance in Medicine, 2022, 88, 2285-2297.	3.0	7
9	Cerebral oxygen extraction fraction (OEF): Comparison of challenge-free gradient echo QSM+qBOLD (QQ) with ¹⁵ 0 PET in healthy adults. Journal of Cerebral Blood Flow and Metabolism, 2021, 41, 1658-1668.	4.3	34
10	Bulk volume susceptibility difference between deoxyhemoglobin and oxyhemoglobin for HbA and HbS: A comparative study. Magnetic Resonance in Medicine, 2021, 85, 3383-3393.	3.0	17
11	Quantification of myocardial oxygen extraction fraction: A proofâ€ofâ€concept study. Magnetic Resonance in Medicine, 2021, 85, 3318-3325.	3.0	2
12	Obesity and White Matter Neuroinflammation Related Edema in Alzheimer's Disease Dementia Biomarker Negative Cognitively Normal Individuals. Journal of Alzheimer's Disease, 2021, 79, 1801-1811.	2.6	18
13	Deep learningâ€based T1â€enhanced selection of linear attenuation coefficients (DLâ€TESLA) for PET/MR attenuation correction in dementia neuroimaging. Magnetic Resonance in Medicine, 2021, 86, 499-513.	3.0	11
14	Pilot study of contrast-free MRI reveals significantly impaired calf skeletal muscle perfusion in diabetes with incompressible peripheral arteries. Vascular Medicine, 2021, 26, 367-373.	1.5	2
15	Deep Image Reconstruction Using Unregistered Measurements Without Groundtruth. , 2021, , .		5
16	Phase2Phase. Investigative Radiology, 2021, 56, 809-819.	6.2	13
17	Cerebral Oxygen Metabolic Stress, Microstructural Injury, and Infarction in Adults With Sickle Cell Disease. Neurology, 2021, 97, e902-e912.	1.1	14
18	Deteriorated regional calf microcirculation measured by contrast-free MRI in patients with diabetes mellitus and relation with physical activity. Diabetes and Vascular Disease Research, 2021, 18, 147916412110290.	2.0	6

#	Article	IF	CITATIONS
19	Evaluation of attenuation correction in PET/MRI with synthetic lesion insertion. Journal of Medical Imaging, 2021, 8, 056001.	1.5	3
20	MR Imaging Differences in the Circle of Willis between Healthy Children and Adults. American Journal of Neuroradiology, 2021, 42, 2062-2069.	2.4	2
21	Harmonization of PET image reconstruction parameters in simultaneous PET/MRI. EJNMMI Physics, 2021, 8, 75.	2.7	2
22	SS-JIRCS: Self-Supervised Joint Image Reconstruction and Coil Sensitivity Calibration in Parallel MRI without Ground Truth. , 2021, , .		2
23	RARE: Image Reconstruction Using Deep PriorsÂLearned Without Groundtruth. IEEE Journal on Selected Topics in Signal Processing, 2020, 14, 1088-1099.	10.8	62
24	Functional Connectivity Decreases with Metabolic Stress in Sickle Cell Disease. Annals of Neurology, 2020, 88, 995-1008.	5.3	11
25	Lesion evolution and neurodegeneration in RVCL-S. Neurology, 2020, 95, e1918-e1931.	1.1	13
26	Optimal co-clinical radiomics: Sensitivity of radiomic features to tumour volume, image noise and resolution in co-clinical T1-weighted and T2-weighted magnetic resonance imaging. EBioMedicine, 2020, 59, 102963.	6.1	63
27	Magnetic resonance safety assessment of a new trend: magnetic eyelashes. Journal of Applied Clinical Medical Physics, 2020, 21, 323-325.	1.9	0
28	Quantification of brain oxygen extraction and metabolism with [150]-gas PET: A technical review in the era of PET/MRI. NeuroImage, 2020, 220, 117136.	4.2	36
29	Bone material analogues for PET/MRI phantoms. Medical Physics, 2020, 47, 2161-2170.	3.0	8
30	Evaluating the Use of rCBV as a Tumor Grade and Treatment Response Classifier Across NCI Quantitative Imaging Network Sites: Part II of the DSC-MRI Digital Reference Object (DRO) Challenge. Tomography, 2020, 6, 203-208.	1.8	12
31	3D pediatric cranial bone imaging using high-resolution MRI for visualizing cranial sutures: a pilot study. Journal of Neurosurgery: Pediatrics, 2020, 26, 311-317.	1.3	13
32	Image Reconstruction for MRI using Deep CNN Priors Trained without Groundtruth. , 2020, , .		4
33	Repeatability of Quantitative Brown Adipose Tissue Imaging Metrics on Positron Emission Tomography with 18F-Fluorodeoxyglucose in Humans. Cell Metabolism, 2019, 30, 212-224.e4.	16.2	21
34	Hydroxyurea reduces cerebral metabolic stress in patients with sickle cell anemia. Blood, 2019, 133, 2436-2444.	1.4	43
35	Measurement Repeatability of ¹⁸ F-FDG PET/CT Versus ¹⁸ F-FDG PET/MRI in Solid Tumors of the Pelvis. Journal of Nuclear Medicine, 2019, 60, 1080-1086.	5.0	23
36	Quantitative MRI of Diffuse Liver Disease: Current Applications and Future Directions. Radiology, 2019, 290, 23-30.	7.3	26

#	Article	IF	CITATIONS
37	Evaluating Multisite rCBV Consistency from DSC-MRI Imaging Protocols and Postprocessing Software Across the NCI Quantitative Imaging Network Sites Using a Digital Reference Object (DRO). Tomography, 2019, 5, 110-117.	1.8	25
38	Increased Cerebral Metabolic Stress Is Associated with Diminished Functional Connectivity in Pediatric Sickle Cell Anemia. Blood, 2019, 134, 989-989.	1.4	0
39	Regional oxygen extraction predicts border zone vulnerability to stroke in sickle cell disease. Neurology, 2018, 90, e1134-e1142.	1.1	81
40	Red cell exchange transfusions lower cerebral blood flow and oxygen extraction fraction in pediatric sickle cell anemia. Blood, 2018, 131, 1012-1021.	1.4	68
41	CAPTURE: Consistently Acquired Projections for Tuned and Robust Estimation. Investigative Radiology, 2018, 53, 293-305.	6.2	12
42	Application of Machine Learning to Automated Analysis of Cerebral Edema in Large Cohorts of Ischemic Stroke Patients. Frontiers in Neurology, 2018, 9, 687.	2.4	34
43	Silent infarcts in sickle cell disease occur in the border zone region and are associated with low cerebral blood flow. Blood, 2018, 132, 1714-1723.	1.4	78
44	Attenuation Correction of PET/MR Imaging. Magnetic Resonance Imaging Clinics of North America, 2017, 25, 245-255.	1.1	75
45	A multi-centre evaluation of eleven clinically feasible brain PET/MRI attenuation correction techniques using a large cohort of patients. NeuroImage, 2017, 147, 346-359.	4.2	200
46	Large-Vessel Vasculopathy in Children With Sickle Cell Disease: A Magnetic Resonance Imaging Study of Infarct Topography and Focal Atrophy. Pediatric Neurology, 2017, 69, 49-57.	2.1	37
47	Comparison of Cerebral Blood Volume and Plasma Volume in Untreated Intracranial Tumors. PLoS ONE, 2016, 11, e0161807.	2.5	10
48	Increased Cortical Cerebral Blood Flow in Asymptomatic Human Immunodeficiency Virus-Infected Subjects. Journal of Stroke and Cerebrovascular Diseases, 2016, 25, 1891-1895.	1.6	10
49	Oximetric angiosome imaging in diabetic feet. Journal of Magnetic Resonance Imaging, 2016, 44, spcone-spcone.	3.4	0
50	TOWERS: Tâ€One with Enhanced Robustness and Speed. Magnetic Resonance in Medicine, 2016, 76, 118-126.	3.0	6
51	Oximetric angiosome imaging in diabetic feet. Journal of Magnetic Resonance Imaging, 2016, 44, 940-946.	3.4	7
52	Reperfusion Beyond 6 Hours Reduces Infarct Probability in Moderately Ischemic Brain Tissue. Stroke, 2016, 47, 99-105.	2.0	11
53	Abstract WMP20: Validation of an Efficient Machine-learning Approach to Quantify CSF Volume Changes Using Multicenter CT Scans. Stroke, 2016, 47, .	2.0	0
54	Correlation Between Cerebral Blood Flow Velocities Measured By Magnetic Resonance and Transcranial Doppler Ultrasound in Children with Sickle Cell Anemia. Blood, 2016, 128, 2496-2496.	1.4	0

#	Article	IF	CITATIONS
55	High-Pressure Transvenous Perfusion of the Upper Extremity in Human Muscular Dystrophy: A Safety Study with 0.9% Saline. Human Gene Therapy, 2015, 26, 614-621.	2.7	16
56	Probabilistic Air Segmentation and Sparse Regression Estimated Pseudo CT for PET/MR Attenuation Correction. Radiology, 2015, 275, 562-569.	7.3	27
57	Defining the Ischemic Penumbra Using Magnetic Resonance Oxygen Metabolic Index. Stroke, 2015, 46, 982-988.	2.0	49
58	MR-based attenuation correction for PET/MRI neurological studies with continuous-valued attenuation coefficients for bone through a conversion from R2* to CT-Hounsfield units. Neurolmage, 2015, 112, 160-168.	4.2	79
59	Hierarchical Reconstruction of 7T-like Images from 3T MRI Using Multi-level CCA and Group Sparsity. Lecture Notes in Computer Science, 2015, 9350, 659-666.	1.3	11
60	Elevations in MR Measurements of Whole Brain and Regional Cerebral Blood Flow and Oxygen Extraction Fraction Suggest Cerebral Metabolic Stress in Children with Sickle Cell Disease Unaffected By Overt Stroke. Blood, 2015, 126, 69-69.	1.4	9
61	Abstract T P45: Automated CSF Segmentation to Quantify Cerebral Edema Following Large Hemispheric Ischemic Stroke. Stroke, 2015, 46, .	2.0	0
62	Noncontrast skeletal muscle oximetry. Magnetic Resonance in Medicine, 2014, 71, 318-325.	3.0	34
63	Tailor the longitudinal anaysis for nih longitudinal normal brain developmental study. , 2014, 2014, 1206-1209.		1
64	Imaging Oxygen Metabolism in Acute Stroke Using MRI. Current Radiology Reports, 2014, 2, 39.	1.4	22
65	Clinically Relevant Reperfusion in Acute Ischemic Stroke: MTT Performs Better than Tmax and TTP. Translational Stroke Research, 2014, 5, 415-421.	4.2	16
66	A pilot study of regional perfusion and oxygenation in calf muscles of individuals with diabetes with a noninvasive measure. Journal of Vascular Surgery, 2014, 59, 419-426.	1.1	26
67	Characteristics of magnetic resonance imaging biomarkers in a natural history study of golden retriever muscular dystrophy. Neuromuscular Disorders, 2014, 24, 178-191.	0.6	46
68	A Generative Model for Resolution Enhancement of Diffusion MRI Data. Lecture Notes in Computer Science, 2013, 16, 527-534.	1.3	4
69	Oxygen Metabolism in Ischemic Stroke Using Magnetic Resonance Imaging. Translational Stroke Research, 2012, 3, 65-75.	4.2	17
70	Noninvasive Measurements of Cerebral Blood Flow, Oxygen Extraction Fraction, and Oxygen Metabolic Index in Human with Inhalation of Air and Carbogen using Magnetic Resonance Imaging. Translational Stroke Research, 2012, 3, 246-254.	4.2	18
71	Early Changes of Tissue Perfusion After Tissue Plasminogen Activator in Hyperacute Ischemic Stroke. Stroke, 2011, 42, 65-72.	2.0	13
72	Signal Evolution and Infarction Risk for Apparent Diffusion Coefficient Lesions in Acute Ischemic Stroke Are Both Time- and Perfusion-Dependent. Stroke, 2011, 42, 1276-1281.	2.0	30

#	Article	IF	CITATIONS
73	Absolute Oxygenation Metabolism Measurements Using Magnetic Resonance Imaging. Open Neuroimaging Journal, 2011, 5, 120-135.	0.2	2
74	Evaluation of MR-Derived Cerebral Oxygen Metabolic Index in Experimental Hyperoxic Hypercapnia, Hypoxia, and Ischemia. Stroke, 2009, 40, 2165-2172.	2.0	59
75	Temporal evolution of cerebral metabolic rate of oxygen utilization using MRI in a middle cerebral artery occlusion stroke. Journal of Cerebral Blood Flow and Metabolism, 2005, 25, S400-S400.	4.3	Ο
76	Impact of intravascular signal on quantitative measures of cerebral oxygen extraction and blood volume under normo- and hypercapnic conditions using an asymmetric spin echo approach. Magnetic Resonance in Medicine, 2003, 50, 708-716.	3.0	116
77	Magnetic resonance cerebral metabolic rate of oxygen utilization in hyperacute stroke patients. Annals of Neurology, 2003, 53, 227-232.	5.3	100
78	Cerebral oxygen extraction fraction and cerebral venous blood volume measurements using MRI: Effects of magnetic field variation. Magnetic Resonance in Medicine, 2002, 47, 958-966.	3.0	121
79	Cerebral venous and arterial blood volumes can be estimated separately in humans using magnetic resonance imaging. Magnetic Resonance in Medicine, 2002, 48, 583-588.	3.0	79
80	Quantitative measurements of cerebral blood flow in patients with unilateral carotid artery occlusion: A PET and MR study. Journal of Magnetic Resonance Imaging, 2001, 14, 659-667.	3.4	107
81	Quantitative measurements of cerebral metabolic rate of oxygen utilization using MRI: a volunteer study. NMR in Biomedicine, 2001, 14, 441-447.	2.8	60
82	Quantitative Measurements of Cerebral Blood Oxygen Saturation Using Magnetic Resonance Imaging. Journal of Cerebral Blood Flow and Metabolism, 2000, 20, 1225-1236.	4.3	198
83	Improving high-resolution MR bold venographic imaging using a T1 reducing contrast agent. Journal of Magnetic Resonance Imaging, 1999, 10, 118-123.	3.4	50